AI-Based Automatic Segmentation of Craniomaxillofacial Anatomy From CBCT Scans for Automatic Detection of Pharyngeal Airway Evaluations in OSA patients

Kaan Orhan (call53@yahoo.com)
Ankara University, Faculty of Dentistry, Department of Dentomaxillofacial Radiology
Mamat Shamshiev
Diagnocat Inc.
Matvey Ezhov
Diagnocat Inc.
Alexander Plaskin
Diagnocat Inc.
Aida Kurbanova
Near East University, Faculty of Dentistry, Department of Dentomaxillofacial Radiology
Gürkan Ünsal
Near East University, Faculty of Dentistry, Department of Dentomaxillofacial Radiology
Maxim Gurasev
Diagnocat Inc.
Maria Golitsyna
Diagnocat Inc.
Seçil Aksoy
Near East University, Faculty of Dentistry, Department of Dentomaxillofacial Radiology
Melis Mısırlı
Near East University, Faculty of Dentistry, Department of Dentomaxillofacial Radiology
Eugene Shumilov
Diagnocat Inc.
Alex Sanders
Diagnocat Inc.
Finn Rasmussen
Internal Medicine Department Lunge Section, SVS Esbjerg, Denmark

Research Article

Keywords: deep learning, artificial intelligence, pharyngeal airway, obstructive sleep apnea, cone-beam computed tomography

Posted Date: December 28th, 2021

DOI: https://doi.org/10.21203/rs.3.rs-1137054/v1

Abstract

This study aims to generate and also validate an automatic detection algorithm for pharyngeal airway on CBCT data using an AI system which will procure an easy, errorless and fast method. The second aim is to validate the newly developed artificial intelligence system in comparison to commercially available software for 3D CBCT evaluation. A Convolutional Neural Network based machine learning algorithm did the segmentation of the pharyngeal airways in OSA and non-OSA patients. Radiologists used a semi-automatic software to manually determine the airway and their measurements were compared with the AI. OSA patients were classified as minimal, mild, moderate and severe groups and the mean airway volumes were compared. Narrowest points (mm), airway areas (mm2) and airway volumes (cc) of both OSA and non-OSA patients were also compared. There was no statistically significant difference between the manual and Diagnocat measurements in all groups ($p>0.05$). According to the results of the Diagnocat and manual segmentation, a successful algorithm which can automatically segment the pharyngeal airway from was created which can be used for a swift and precise measurement of pharyngeal airway volume.

Introduction

Obstructive sleep apnea (OSA) is identified by periods of partial or complete upper airway disruption during sleep. Hypoxemia, retention of carbondioxide, alteration in the autonomic structure and hemo-dynamic responses are induced by OSA [1]. OSA patients who does not receive any treatment may have hypertension, heart failure, stroke, and premature death [2]. OSA patients are unavailable to preserve the pharyngeal airway space when they sleep, however, they can breathe normally when they are awake [3].

Inferior displacement of hyoid bone, mandibular insufficiency and increased soft palate and tongue volume are described in OSA patients by researchers in the literature [4]. The location of the collision is generally located posterior to the soft palate, tongue, uvula or combination of these structures [5]. Frequent reasons for collapsing of the upper airway are described as the; the competence of the airway by reflexes, pharyngeal inspiratory muscle activity, anatomic contraction of the upper airway [6]. Since the diagnosis of OSA requires a multidisciplinary approach, a dentist, a neurologist, a cardiologist, a otorhinolaryngologist and a pulmonary medicine specialist should be involved [7].

CBCT is a 3-Dimensional radiographic diagnostic unit which can scan a region of interest with superior definition image acquisition. This can provide a thorough analysis of the bony structures which are determinant in OSA patients [8]. Due to its

lower dose, cost and higher image quality, CBCT is preferred over other 3D imaging methods such as conventional CT in dentistry especially for the evaluation of the craniofacial structures [9].

Despite not having common applications in orthodontics and other departments of the dentistry, AI has provided brilliant results in cephalometric analysis for determination of maturation staging of the cervical vertebras, tooth extraction decision and facial structure evaluation in patients who had been treated for cleft palate [10, 11].

Anatomical structures such as craniofacial skeleton and soft tissues which surround the muscles and pharynx have a crucial role in the configuration of the upper airway. Pharynx morphology is known to be one of the major factors that may cause OSA. Air-flow obstruction in children is also thought to be occur due to skeletal deficiency since the contraction in the anterior-posterior aspect of the airway ensue from the positioning of the mandible and maxilla [12–14].

Numerous softwares are available in order to analyze the CBCT data with semi-automatic or manual volumetric measurement process [15]. However most of those softwares are laborious, time-consuming and a completely automatic airway detection algorithm is limited [11]. Thus, the aim of this is to generate and also validate an automatic detection algorithm for pharyngeal airway on OSA patient's CBCT data using an artificial intelligence system that will provide an easy, errorless and fast method. The second aim is to validate the newly developed artificial intelligence system in comparison to commercially available software for 3D CBCT evaluation.

Materials And Methods

Written informed consent was obtained from all patients before their radiographic examinations. The research protocol was performed following the principles of the Declaration of Helsinki and was approved by the non-interventional Institutional Review

Board (IRB) of our university's Health Sciences Ethics Committee. Deidentification was performed in compliance with the Information Commissioner's Anonymization: managing data protection risk code of practice (https://ico.org.uk/media/1061/anonymisation-code.pdf*)*, and validated by the aforementioned institution. This study does not contain any active involvement of the patients. The study data was created only from the deidentified anonymized data.

Anonymized DICOM files of the CBCT images which were taken by 3 different CBCT units were used in this study. The CBCT units were Pax-i3D Smart PHT-30LFO0 (Vatech, South Korea), Carestream Health CS 8100 3D (Kodak, USA), Orthophos XG 3D (Sirona, Germany). Images were obtained using up to 120mm × 90mm FOV between. All CBCT units have isotropic voxels which differs between 0.1 mm^3 to 0.2 mm^3.

The primary aim of this study was to generate an AI algorithm for segmentation of craniomaxillofacial anatomy and second to test this algorithm for automatic detection algorithm for pharyngeal airway bot for OSA and control patients. Thus, this study has two notable parts as dataset preparation for the evaluation and to test the practicability of the system in order to enhance the diagnostic capabilities

CBCT anatomy localization generated with AI model

Approach

To handle large volume sizes on a reasonably fine scale, we approach this task with a coarse-to-fine framework, where the whole volume is first analyzed as semantic segmentation in coarse resolution, followed by a patch-based semantic segmentation with a coarse hint in fine resolution. Our approach to training the system consists of the following steps: Preprocessing incoming volumetric image; coarse model training; coarse hint generation; patch-based training in fine resolution with a hint from the coarse model.

Data

We use a simple min-max normalization within a fixed window. We clip the intensities to be inside the [-1000, 2000] interval, then subtract a minimum intensity value and divide by a maximum one. Different methods have also been examined. According to our experiments, the training procedure is not sensitive to the choice of preprocessing and all methods lead to approximately the same results. The data is split into training, development and test sets. We use 90% of the data for training, 5% for the development set and 5% for the test set.

For the Coarse step, we rescale the image to have 1.0mm isotropic voxel resolution using linear interpolation. To provide the Coarse model more information, we obtain soft coarse segmentation ground truth labels by the following procedure. First, we encode the original semantic segmentation mask of shape DxHxW with a one-hot encoding scheme which results in a tensor of shape tensor CxDxHxW, where C represents number of classes and D, H, W are the spatial dimensions of the original volume. Next, we use linear interpolation to rescale this tensor to have a 1.0mm resolution. The resulting tensor consists of the probability distributions over classes for each spatial position and is referred to as soft targets.

For the Fine step, the target voxel spacing of the model is 0.25 x 0.25 x 0.25mm which is also achieved with linear interpolation of the image. For this step, we obtain the ground truth labels via a simple nearest neighbour downsampling of original semantic segmentation masks. During training, we randomly sample patches of size 144 x 144 x 144 voxels.

Model

We formulate both Coarse and Fine steps as a semantic segmentation task, where the background and each anatomical element is interpreted as a separate class. For both Coarse and fine steps, we exploit a same pre-trained semantic segmentation network based on internally modified fully convolutional 3D U-Net architecture [16].

Since the Fine model is trained using a patch-based approach, it's crucial to provide the model with global information. We achieve it by utilizing a coarse hint. A coarse hint is the Coarse model output which is interpolated to the Fine-scale and passed to the Fine model as additional input channels. To prevent possible data leakage, we train the Coarse model and prepare coarse hints via three-fold cross-validation. Therefore, the only difference between the Coarse and Fine models architectures is the number of input channels: for the Coarse step it equals 1, and for the Fine step it equals the number of classes plus 1.

The class imbalance is known to be a challenging problem in medical semantic segmentation tasks. We approach this issue by using a sum of a standard cross-entropy loss and soft multiclass Jaccard loss. To prevent overfitting and enhance the performance of the model we also utilize a large variety of data augmentations. For the Coarse step the following augmentations are used during training: random blur, random noise, random rotations, random scaling, random crops, random elastic deformation, random anisotropy [16]. For the Fine step, we used the same set of augmentations except for random elastic deformation and random anisotropy since these transformations are computationally expensive when applied to reasonably large images.

Training

To sum it up, our training procedure consists of the following steps. First, we train the Coarse model on the coarse training dataset with soft targets. This checkpoint is used during the testing. We also perform three-fold cross-validation and use the obtained checkpoints later to generate coarse hints for the Fine step. For both cross-validation and full data training, we followed the same procedure. We train for a total of 100 epochs using Adam optimizer with a one-cycle scheduling policy with a maximum learning rate equal to 1e-3, minimum learning rate equal to 1e-6, 0.05 warmup fraction and a batch size of 1.

Next, we prepare coarse hints for the Fine model. We utilize the checkpoints received via cross-validation and make out-of-folds predictions, then linearly interpolate the output probability maps to the Fine model voxel spacing and concatenate them with the original intensity value channel. Finally, we train the Fine model for a total of 40 epochs, using Adam optimizer and the same learning rate scheduling policy, as in the Coarse step.

To train the Fine model we use a patch-based approach. At the beginning of the training epoch, we iterate over the images, randomly sample 20 patches per volume and store them in a queue of size 180. Once the queue has reached a specified maximum length we start to retrieve the random patches from it and pass them to the network while simultaneously preparing new patches and adding them to the queue. For evaluation, we use the checkpoint with the lowest recorded validation loss for both Coarse and Fine models.

Implementation

Our algorithm was based on Python implementation of U-net. All training and experiments were done using NVIDIA® GeForce® RTX A100 GPU. Adam optimizer was used for the network training.

Inference

At test time the patch-based approach is known to produce the predictions of a worse quality near the borders of the output patch. To alleviate this issue, we perform inference in overlapping patches and aggregate the predictions with weights which make the centre voxel of an output patch contribute more to the final result than its borders. We set the patches' overlap to 16 (Figure 1).

Patient test dataset

To estimate the generalizability of our model, a retrospective patient CBCT dataset from Dentomaxillofacial Radiology Department in Near East University was used. A power analysis was conducted with a statistical power of 90%, the significance level of 0.05 α, and a probability of type II error as 0.2 β. A minimum number of 82 CBCT images for both control and OSA groups were required according to the power analysis.

Hence, our study was conducted with randomly selected artefact-free 100 OSA and 100 control CBCT images existing in our faculty's database. All patients provided their informed consent before irraditation, and the consent forms were reviewed and approved by the institutional review board of the faculty. Exclusion criteria were evident skeletal asymmetries, cleft palate, cleft lip, current ongoing orthodontic treatment, any teeth that overlie apical region of the incisors.

The dataset of a previous study of ours is used in this study [17]. "CBCT records of 200 patients (100 images of OSA patients and 100 images of the control group) were retrospectively collected and analyzed along with the polysomnography records and body mass index (BMI) of OSA patients at the Department of Allergy, Sleep and Respiratory Diseases. AHI is the number of apnea + hypopnea seen each hour during sleep. Sleep apnea severity was evaluated in 4 different subtypes as minimal, mild, moderate and severe. Patients with Apnea-Hypopnea Index(AHI) value lower than 5 were classified as minimal group while patients with AHI values between 5-15, 15-30 and more than 30 were classified as mild, moderate and severe, respectively. 100 OSA patients had symptoms of this disease and evaluation of these patients was accomplished by a standardized program at the Department of Allergy, Sleep and Respiratory Diseases, which also consists of anthropometric measurements, dental examination, CBCT and polysomnography.

Polysomnography uses various methods like electroencephalography, electromyogram, electro-oculography, respiratory effort measurement, airflow measurement and snoring [12]. Control (non-OSA) patients had none of the clinical findings of the OSA patients such as snoring, dyspnea, witnessed apnea, coughing or daytime sleepiness. So their images were used as a control group. The mean age for OSA patients was 53.2 years and for non-OSA patients was 46.4 years. Principles characterized in the Declaration of Helsinki were applied during the protocol of study along with modifications and revisions.

CBCT images of the test group were obtained by NewTom 3 G Quantitive Radiology s.r.l., (NewTom, Verona, Italy). CBCT records for non-OSA patients had been taken for implant planning, evaluation of impacted teeth, prosthodontic and orthodontic purposes. Patients with osteoporosis, skeletal asymmetries and medication related bony alterations were excluded from the study.

Ground truth segmentation process

All CBCT data was exported as DICOM files and then anonymized. The axial, coronal and sagittal slices were oriented in order to ensure a proper evaluation. The axial slices were aligned with maintaining the palate line and the ground perpendicular to each other. Coronal slices were oriented with aligning the both orbits and midline of the head parallel to the ground and the sagittal slices were aligned with linear orientation of the ANS and PNS.

All CBCT images had been segmented prior to our study to be used for diagnosis, pharyngeal airway evaluations and surgical planning using InVivo 5.1.2 ® (*Anatomage Inc., San Jose, CA, USA*). DICOM files of the axial CBCT images were exported with a 512 x 512 matrix and were imported to InVivo 5.1.2. In this software, the evaluation of the pharyngeal airway can be measured both automatic thresholding and manual tracing with semiautomatic thresholding.

The pharyngeal airway is originated by the nasopharynx and the oropharynx. In order to assess the borders of the oropharyngeal airway volume, ANS-PNS plane which extends to the wall of pharynx was determined as the superior border and the most inferior-anterior point of the 2nd cervical vertebrae which is parallel to the superior border was determined as the lower border of the oropharyngeal airway. Since the superior border of the oropharyngeal airway is also the lower border of the nasopharyngeal airway, a line perpendicular from the PNS to the palatal plane is drawn in order to form the anterior border of the nasopharyngeal airway. Sum of the nasopharyngeal airway and oropharyngeal airway is calculated with both manual tracing with semi-automatic thresholding and automatic thresholding in InVivo 5.1.2. viewer. S.A. and A.K. observed the CBCT images twice with a week interval to avoid any intra-observer disagreement for ground truth measurement.

For automatic thresholding, the software itself detects the pharyngeal airway volume, area narrow point area and measure the narrow point automatically (Figure 2).

The manual tracing with semiautomatic thresholding was done by cropping the airway using the “edit masks” feature and the connection with the outer air was cropped in each slice with the segmentation tools. The “region growing” tool was used in order to split the segmentation produced by thresholding into several objects and to remove floating pixels an the pharyngeal airway volume and area were calculated using the “calculate 3D” tool feature of the software (Figure 3, Figure 4A-B).

3D U-Net architecture framework (AI model)

Our approach is automatic segmentation focusing on the regions of interest: the external surface of the bones, teeth and airways. This process results in 5 segmentation masks as the upper skull, the mandible, maxillary teeth, mandibular teeth and the airways. We performed a series of trials to choose the best training configuration. Following, the generated stl files were downloaded and imported to 3rd party software for volumetric pharyngeal airway measurements (*3-Matic Version 15, Materialise*) (Figure 5).

Statistical Analysis

Statistical analysis was performed using SPSS 22.0 software (*SPSS Inc., Chicago, IL, USA*). Due to the non-normal distribution of the data, the Mann-Whitney U test was used for comparisons between paired groups and the Kruskall Wallis H test was used for comparisons between three or more groups. Significance level was set as 0.05 and it was stated that there was a significant difference in case of $p<0.05$, and no significant difference in case of $p>0.05$.

Results

There were no statistically significant airway volume (cc) measurement difference between the manual technique and Diagnocat (DC) in all OSA severity subtypes (p>0.05). p values were 0.052, 0.942, 0.642 and 0.207 for the minimal, mild, moderate and severe OSA groups, respectively. The highest difference was found in the minimal OSA group (Table 1).

There was no statistically significant difference in narrowest points (mm), airway area (mm^2) and total airway volume (cc) measurements between the manual and DC in Non-OSA patients. p values were 0.346, 0.111 and 0.667, respectively. The mean value for the narrowest distance was found 5.96mm with the manual technique and 5.70mm with DC. The mean value for the airway area was found 883.41mm^2 with the manual technique and 930.02mm^2 with DC. The mean value for the total airway volume was found 17.95cc with the manual technique and 18.50cc with DC (Table 2).

There were, also, no statistically significant difference in narrowest points (mm), airway area (mm^2) and total airway volume (cc) measurements between the manual and DC in OSA patients. p values were 0.931, 0.305 and 0.139, respectively. The mean value for the narrowest distance was found 6.31mm with the manual technique and 6.10mm with DC. The mean value for the airway area was found 1057.59mm^2 with the manual technique and 1013.90mm^2 with DC. The mean value for the total airway volume was found 19.63cc with the manual technique and 20.25cc with DC (Table 3).

Discussion

According to our review of the literature, this study is the first study that automatically mesaured the pharyngeal airway in OSA patients. However, manual measurements of the pharyngeal airway in OSA patients and automatic mesaurements of the pharyngeal airway in Non-OSA patients are present in the literature. Since the studies demonstrated that the pharyngeal airway volume is significantly lower and the morphology is dissimilar in mouth breathers than in nasal breathers, deep learning algorithms which concenrate on airway volume measurements should be trained and tested with various data. In orthodontics, airway volume and the underlying factors play a crucial role before orthognathic surgery planning, analyzing the airway volume is indispensable to understand the oral and pharyngeal adjustments to vicissitudinous respiratory conditions [11, 18–20].

Various authors measured the airway in adults and according to their results it is fair to state that the difference between their measurements have occured due to human factor during the segmentation and measurement and different softwares that is used during the measurements. Furthermore, in order to compare the success and accuracy of the other studies, the airway boundaries should be exactly and identically determined [11, 21, 22].

It is a well known fact that automated segmentations will aid the orthodontics in routine clinical workflow with the treatment plan and airway measuremets with reducing the segmentation time and removing the inter-practioner measurement and interpretation differences [11].

There are three limitations to this study:

- **Image acquisition protocols**. All CBCT images which were used in this study were obtained by a single CBCT unit with identical acquisition protocol. In order to achieve an unbiased accuracy rate, data by multiple CBCT units should be used.
- **Single centre data.** In the literature it has been widely suggested that randomized controlled studies should be performed with multi centre data in order to eliminate the bias. Unfortunately, our data was only obtained from our university.
- **Limited Soft tissue contrast**. Arranging a Hounsfield Unit threshold in CBCT images could not be done precisely in the segmentation process which will affect the airway volume.

Declarations

Acknowledgment

Since the present study have been conducted by the retrospective radiologic images, it is not subject to the "registration" and "clinical trial number" procedures required for clinical trials (Clinical Trials or Observational Studies)

Competing Interests : “Financial support was received by Diagnocat Co. Ltd., San Francisco CA. Matvey Ezhov, Maxim Gusarev, Alexander Plaskin, Mamat Shamshiev, Maria Golitsyna, Eugene Shumilov, and Alex Sanders are employees of Diagnocat Co. Ltd.

Kaan Orhan is a scientific research advisor for the Diagnocat Co. Ltd., Aida Kurbanova, Melis Misirli, Gürkan Ünsal, Secil Aksoy, Finn Rasmussen have no potential competing interests."

Author contributions : K.O. designed the work and interpreted the data. A.K, G.Ü., S.A., F.R. and M.M. interpreted the data and were responsible of the data acquisition and analysis. M.E., M.G., M.G., E.S. and A.S., created a new software for this study. K.O. and G.Ü. drafted the work and all authors contributed or revised it. All authors agreed both to be personally accountable for the author's own contributions and to ensure that questions related to the accuracy or integrity of any part of the work, even ones in which the author was not personally involved, are appropriately investigated, resolved, and the resolution documented in the literature.

References

1. Salles, C., et al., Obstructive sleep apnea and asthma. J Bras Pneumol, 2013. 39(5): p. 604–12.
2. Ogna, A., et al., Obstructive Sleep Apnea Severity and Overnight Body Fluid Shift before and after Hemodialysis. Clin J Am Soc Nephrol, 2015. 10(6): p. 1002–10.
3. Dempsey, J.A., et al., Pathophysiology of sleep apnea. Physiol Rev, 2010. 90(1): p. 47–112.
4. Drakatos, P., et al., Computed tomography cephalometric and upper airway measurements in patients with OSA and erectile dysfunction. Sleep Breath, 2016. 20(2): p. 769–76.
5. White, D.P. and M.K. Younes, Obstructive sleep apnea. Compr Physiol, 2012. 2(4): p. 2541–94.
6. Hudgel, D.W., Mechanisms of obstructive sleep apnea. Chest, 1992. 101(2): p. 541–9.
7. Oz, U., et al., Association between pterygoid hamulus length and apnea hypopnea index in patients with obstructive sleep apnea: a combined three-dimensional cone beam computed tomography and polysomnographic study. Oral Surg Oral Med Oral Pathol Oral Radiol, 2016. 121(3): p. 330–9
8. von Arx, T., et al., Evaluation of location and dimensions of lingual foramina using limited cone-beam computed tomography. J Oral Maxillofac Surg, 2011. 69(11): p. 2777–85.
9. Sheikhi, M., F. Mosavat, and A. Ahmadi, Assessing the anatomical variations of lingual foramen and its bony canals with CBCT taken from 102 patients in Isfahan. Dent Res J (Isfahan), 2012. 9(Suppl 1): p. S45-51.
10. 10.. Amasya, H., et al., Validation of cervical vertebral maturation stages: Artificial intelligence vs human observer visual analysis. Am J Orthod Dentofacial Orthop, 2020. 158(6): p. e173-e179.
11. Sin, C., et al., A deep learning algorithm proposal to automatic pharyngeal airway detection and segmentation on CBCT images. Orthod Craniofac Res, 2021.
12. Rundo, J.V. and R. Downey, 3rd, Polysomnography. Handb Clin Neurol, 2019. 160: p. 381–392.
13. Avci, S., et al., Relationships among retropalatal airway, pharyngeal length, and craniofacial structures determined by magnetic resonance imaging in patients with obstructive sleep apnea. Sleep Breath, 2019. 23(1): p. 103–115.
14. Stellzig-Eisenhauer, A. and P. Meyer-Marcotty, Interaction between otorhinolaryngology and orthodontics: correlation between the nasopharyngeal airway and the craniofacial complex. GMS Curr Top Otorhinolaryngol Head Neck Surg, 2010. 9: p. Doc04.
15. Park, C.W., et al., Volumetric accuracy of cone-beam computed tomography. Imaging Sci Dent, 2017. 47(3): p. 165–174.
16. Pérez-García, Fernando, Rachel Sparks, and Sebastien Ourselin. "TorchIO: a Python library for efficient loading, preprocessing, augmentation and patch-based sampling of medical images in deep learning." Computer Methods and Programs in Biomedicine (2021): 106236.
17. Firincioglulari M, Aksoy S, Orhan K, Oz U, Rasmussen F. Comparison of anterior mandible anatomical characteristics between obstructive sleep apnea patients and healthy individuals: a combined cone beam computed tomography and polysomnographic study. Eur Arch Otorhinolaryngol. 2020;277(5):1427–1436. doi:10.1007/s00405-020-05805-2
18. Pinheiro de Magalhaes Bertoz, A., et al., Three-dimensional airway changes after adenotonsillectomy in children with obstructive apnea: Do expectations meet reality? Am J Orthod Dentofacial Orthop, 2019. 155(6): p. 791–800.
19. Alves, M., Jr., et al., Three-dimensional assessment of pharyngeal airway in nasal- and mouth-breathing children. Int J Pediatr Otorhinolaryngol, 2011. 75(9): p. 1195–9.
20. Cuccia, A.M., M. Lotti, and D. Caradonna, Oral breathing and head posture. Angle Orthod, 2008. 78(1): p. 77–82.

21. Hong, J.S., et al., Three-dimensional analysis of pharyngeal airway volume in adults with anterior position of the mandible. Am J Orthod Dentofacial Orthop, 2011. 140(4): p. e161-9.
22. Grauer, D., et al., Pharyngeal airway volume and shape from cone-beam computed tomography: relationship to facial morphology. Am J Orthod Dentofacial Orthop, 2009. 136(6): p. 805–14.

Tables

Table 1: Comparison of the airway volume mesaurements of Diagnocat and manual technique in patients with different OSA severities.

	OSA Severity	Technique (Subgroup)	Mean	Median	min	max	sd	Mann Whitney U		
								Mean Rank	U	p
Airway Volume (cc)	Minimal OSA	Manual	21,18	21,03	11,81	34,87	6,49	31,67	252	0,052
		DC	17,73	16,20	7,60	29,60	6,16	23,33		
		Total	19,45	19,66	7,60	34,87	6,51			
	Mild OSA	Manual	18,32	17,72	7,64	28,46	6,23	19,63	178	0,942
		DC	18,11	17,60	7,70	29,50	6,18	19,37		
		Total	18,22	17,66	7,64	29,50	6,12			
	Moderate OSA	Manual	22,42	22,55	9,69	35,53	7,45	22,38	202	0,642
		DC	21,42	21,20	6,60	35,30	6,96	20,62		
		Total	21,92	21,92	6,60	35,53	7,14			
	Severe OSA	Manual	19,21	17,85	7,34	34,97	7,54	36,48	446	0,207
		DC	16,79	15,20	5,60	29,60	6,73	30,52		
		Total	18,00	15,72	5,60	34,97	7,20			

Table 2: Comparison of airway volume, airway area and narrowest line of the airway measurements of Diagnocat and manual technique in patients without OSA

Non-OSA patients											
		n	Mean	Median	Minimum	Maximum	sd	Mean Rank	U	p	Test
Points (mm)	Narrow	100	5,96	5,58	1,89	13,30	2,07	104,36	4614,5	0,346	Mann-Whitney U
	DC Narrow	100	5,70	5,41	1,69	14,56	2,10	96,65			
	Total	200	5,83	5,46	1,69	14,56	2,08				
Area (mm^2)	Total Airway	100	883,41	856,73	437,65	1576,88	212,92	93,97	4347	0,111	Mann-Whitney U
	DC Total Airway	100	930,02	909,00	597,33	1694,00	201,18	107,03			
	Total	200	906,71	895,67	437,65	1694,00	207,93				
Volume(cc)	Total Airway	100	17,95	17,70	4,90	34,10	5,45	146,12	0,811	0,667	Kruskall-Wallis H
	Manual Total Airway	100	18,50	18,40	5,50	35,20	5,63	156,71			
	DC Airway	100	17,96	18,20	4,80	32,80	5,41	148,68			
	Total	300	18,14	18,00	4,80	35,20	5,48				

Table 3: Comparison of airway volume, airway area and narrowest line of the airway measurements of Diagnocat and manual technique in patients with OSA

OSA patients											
		n	Mean	Median	Minimum	Maximum	sd	Mean Rank	U	p	Test
Points (mm)	Narrow	100	6,31	5,86	1,48	23,08	3,42	100,14	4964	0,931	Mann-Whitney U
	DC Narrow	100	6,10	5,76	1,01	19,90	2,50	100,86			
	Total	200	6,20	5,78	1,01	23,08	2,99				
Area (mm^2)	Total Airway	100	1057,59	1033,07	598,85	1731,64	244,38	104,70	4580	0,305	Mann-Whitney U
	DC Toplam Airway	100	1013,90	989,81	466,52	1670,22	256,57	96,30			
	Total	200	1035,74	1001,13	466,52	1731,64	250,88				
Volume(cc)	Total Airway	100	19,63	19,05	7,40	35,30	6,90	153,05	3,9	0,139	Kruskall-Wallis H
	Manual Total Airway	100	20,25	19,83	7,34	35,53	7,08	161,21			
	DC Airway	100	18,27	17,50	5,60	35,30	6,65	137,24			
	Total	300	19,38	18,55	5,60	35,53	6,91				

Figures

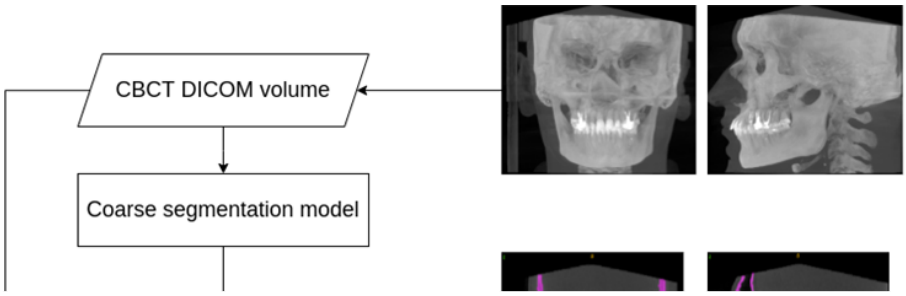

Figure 1

Inference algorithm

Figure 2

Automatic thresholding and the detection of the pharyngeal airway volume, area and narrow points.

Figure 3

“Calculate 3D” tool of the Diagnocat software for pharyngeal airway area

Figure 4

A-B: “Calculate 3D” tool of the Diagnocat software for pharyngeal airway volume

Figure 5

3-Matic’s interface for volumetric pharyngeal airway measurements